LCLS-TN-04-13
SLAC–PUB–10763
September, 2004

Emittance and Quantum Efficiency Measurements from a 1.6 cell S-Band Photocathode RF Gun with Mg Cathode*

J.F. Schmerge, J.M. Castro, J.E. Clendenin, D.H. Dowell, S.M. Gierman, and R.O. Hettel
Stanford Linear Accelerator Center, Stanford University, Stanford, California 94309

Abstract

A comparison of electron beam parameters from a 1.6 cell S-band rf gun with Cu and Mg cathode at the SLAC Gun Test Facility are reported. The lower work function of Mg compared to Cu theoretically increases the quantum efficiency for a fixed laser wavelength and also increases the thermal emittance. Slice emittance measurements at low charge (15 pC) set an upper limit on the thermal emittance of 0.6 and 1.2 microns per mm radius for the Cu and Mg cathodes respectively. The longitudinal emittance measurements with both cathodes exhibit large energy spreads emitted from the gun. The measured quantum efficiency with no laser cleaning is approximately 3 10^{-5} at 110 MV/m and 30° laser phase for the Cu and 8 10^{-5} at 90 MV/m and 30° laser phase for the Mg cathode.

Submitted to 26th International Free-Electron Laser Conference
8/29/2004—9/3/2004, Trieste, Italy

* Work supported by Department of Energy contract DE–AC02–76SF00515.

EMITTANCE AND QUANTUM EFFICIENCY MEASUREMENTS FROM A 1.6 CELL S-BAND PHOTOCATHODE RF GUN WITH MG CATHODE

J.F. Schmerge*, J.M. Castro, J.E. Clendenin, D.H. Dowell, S.M. Gierman, and R.O. Hettel, SLAC, Menlo Park, CA 94025, USA

Abstract

A comparison of electron beam parameters from a 1.6 cell S-band rf gun with Cu and Mg cathode at the SLAC Gun Test Facility are reported. The lower work function of Mg compared to Cu theoretically increases the quantum efficiency for a fixed laser wavelength and also increases the thermal emittance. Slice emittance measurements at low charge (15 pC) set an upper limit on the thermal emittance of 0.6 and 1.2 microns per mm radius for the Cu and Mg cathodes respectively. The longitudinal emittance measurements with both cathodes exhibit large energy spreads emitted from the gun. The measured quantum efficiency with no laser cleaning is approximately 3 10^{-5} at 110 MV/m and 30° laser phase for the Cu and 8 10^{-5} at 90 MV/m and 30° laser phase for the Mg cathode.

INTRODUCTION

The cathode is one of the most important components of a photocathode rf gun as it defines the quantum efficiency (QE) and the minimum achievable emittance or so called thermal emittance. In addition the cathode also affects the maximum attainable field in the gun due to rf breakdown at the cathode to back plate joint. The ideal cathode would exhibit high QE, low thermal emittance and would not limit the maximum attainable field. A peak on axis field of 120 MV/m is required in order to achieve an emittance of 1 μm with 1 nC of charge as desired for the Linac Coherent Light Source (LCLS) [1]. The maximum required field limits the choice of cathode materials to metals.

This paper reports the results of measurements made at the SLAC Gun Test Facility with a Mg cathode. The results are also compared with theoretical values and previously reported Cu cathode results [2]. The Cu cathode used in the study is a 1 cm diameter, single crystal (100 orientation) brazed into the polycrystalline Cu back plate. After brazing, the cathode was polished with 0.25 μm diamond paste and installed on the gun in a N_2 environment. The 2 cm diameter Mg insert was friction welded into the Cu back plate. After welding, the Mg cathode and back plate surface were machined using single point diamond tools. The cathode was offset from the lathe center to eliminate a machining defect at the center of the cathode. The Mg cathode was installed on the gun in air so that the electric field on axis could be measured with a bead drop measurement.

The maximum field attained with the Cu cathode was 127 MV/m with reliable operation at 110 MV/m and typically 2 10^{-9} Torr vacuum pressure during electron beam operation. The Mg cathode was limited to lower fields due to rf breakdown. The maximum field achieved was 107 MV/m with reliable operation at 95 MV/m and 5 10^{-10} Torr vacuum pressure with electron beam. For comparison, a polycrystalline Cu cathode with no braze or weld joint was operated up to 140 MV/m with reliable operation at 125 MV/m.

*schmerge@slac.stanford.edu

THEORY

The definition of thermal emittance is shown in equation 1 where x is the beam position and p_x is the transverse momentum [3]. Assuming a flat transverse laser pulse shape and averaging over the electron energy distribution leads to equation 2 where $r_{cathode}$ is the laser beam radius, E_k is the electron kinetic energy in the metal given by the sum of the Fermi energy and photon energy and E_b is the metal barrier energy which is the sum of the Fermi energy and work function less the Schottky barrier reduction. Using the definition of QE as the number of emitted electrons per incident photons, the QE can be computed as shown in equation 3 where R is the optical reflectivity. After integration the QE simplifies to equation 4 where E_F is the Fermi energy.

$$\varepsilon_{n-thermal} \equiv \frac{1}{mc}\sqrt{\langle x^2\rangle\langle p_x^2\rangle} \tag{1}$$

$$\varepsilon_{nthermal} = \frac{r_{cathode}}{2}\sqrt{\frac{2E_k}{mc^2}}\sqrt{\frac{\left(1-\left(E_b/E_k\right)^2+2\left(E_b/E_k\right)^{3/2}-2\left(E_b/E_k\right)^{1/2}\right)}{6\left(1+\left(E_b/E_k\right)-2\left(E_b/E_k\right)^{1/2}\right)}} \tag{2}$$

$$QE \equiv (1-R)\frac{\int_{E_{\min}}^{E_b}\int_0^{\cos^{-1}\sqrt{\frac{E_b}{E+E_{photon}}}}\int_0^{2\pi} N_{electron}\sin\Phi d\theta d\Phi dE}{\int_0^{E_b}\int_0^{\pi}\int_0^{2\pi} N_{electron}\sin\Phi d\theta d\Phi dE} \tag{3}$$

$$QE = (1-R)\frac{\left(1+\left(E_b/E_k\right)-2\left(E_b/E_k\right)^{1/2}\right)}{2\left(E_F/E_k\right)} \tag{4}$$

Thermal emittance is primarily a function of the Fermi energy, work function and photon energy. The quantum efficiency depends on the same parameters and is also dependent on the optical reflectivity. The Cu and Mg cathode parameters are listed in Table 1 along with the calculated skin depth, QE and thermal emittance for 263 nm (4.71 eV) normal incidence photons. For the calculation it is assumed the Cu cathode has a 110 MV/m

rf field with 30° laser phase and 90 MV/m, 30° is assumed for the Mg cathode.

Table 1: Cathode parameters assuming 4.71 eV photons at normal incidence.

Parameter	Cu	Mg	Units
Work Function	4.59 [4]	3.66 [4]	eV
Fermi Energy	8.7 [5]	7.1 [5]	eV
Power Reflectivity	34 [6]	92 [7]	%
Skin depth	25	19	nm
QE	11	21	10^{-5}
$\varepsilon_{n\text{-thermal}}$	0.25	0.46	μm

The equations have been derived assuming a flat cathode surface at absolute zero and electron-electron scattering is ignored. Operation at room temperature increases the reported thermal emittance and QE for the Cu cathode by less than 2%. Temperature effects become significant above about 300 C for Cu and approximately 2000 C for Mg. The inelastic mean free path (IMFP) for electrons in Cu and Mg at 4.7 eV above the Fermi energy is not well documented. From the literature the IMFP is estimated to be on the order of 5 nm [5,8]. Since the mean free path is less than the skin depth it must be included for good agreement between theory and experiment. Including scattering will reduce the calculated QE and thermal emittance as it will decrease the average energy of photo-emitted electrons. Surface roughness has two effects. First, sharp surface features cause field enhancement that increase the Schottky effect and thus the QE and thermal emittance. Second, since electrons are emitted from a narrow cone with respect to the surface normal [3], roughness also affects the angular distribution. This effect increases the thermal emittance but has no effect on the QE. Both effects are localized and must be averaged over the entire cathode.

MEASUREMENTS

The measurements reported here are performed with a nearly Gaussian temporal pulse shape with approximately 2 ps FWHM duration. The transverse laser shape is flat and unless otherwise noted the radius is 1 mm. The laser is incident on the cathode at near normal incidence. The Cu cathode was operated at 110 MV/m and 30° laser phase resulting in 5.7 MeV beam exiting the gun. The Mg cathode was operated at 95 MV/m with 30° laser phase resulting in 5.0 MeV beam unless otherwise noted. All measurements are made with 15 pC of charge corresponding to about 12 A of peak current unless otherwise noted.

Quantum Efficiency

The QE is determined by measuring the laser energy incident on the cathode with a Joule meter and the charge exiting the gun on an insertable Faraday cup immediately downstream of the gun. The measured QE versus the laser phase for both cathodes is shown in figure 1. The QE from the Mg cathode exhibits less phase dependence than the Cu cathode because the Schottky effect is less significant due to the lower work function.

In an attempt to increase the QE from the Mg cathode, a high intensity laser pulse was scanned across the cathode with the rf off. A lens was inserted in the drive laser beam path which reduced the 2 mm diameter beam to a 68 μm rms spot size. The maximum energy available at the cathode was 22 μJ resulting in a maximum fluence at the cathode of 800 μJ/mm^2. With the maximum fluence incident on the cathode there was no observable change in the vacuum pressure. Likewise there was no measurable increase in QE after the laser cleaning attempt. No attempt was made to laser clean the Cu cathode.

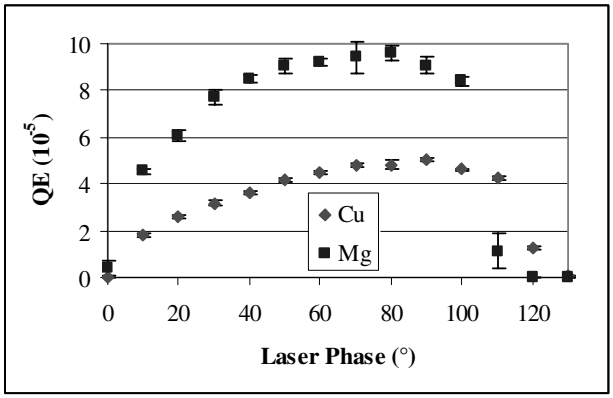

Figure 1: The QE versus laser phase. The peak field at the cathode is 110 MV/m for Cu and 90 MV/m for Mg.

The variation of QE across the cathode was also measured by scanning a 130 μm rms laser beam over a 1.5 X 1.5 mm area on the Mg cathode. The rms QE variation was 83% of the average and the minimum and maximum QE were 44% and 660% of the average respectively. The variation is probably due to localized surface contaminants either lowering the work function or altering the optical reflectivity. Since the Schottky effect is less significant for the Mg cathode it is unlikely the variation is caused by rf field enhancement due to localized sharp features on the cathode. The QE uniformity was significantly improved approximately 0.7 mm off center. Thus the laser was intentionally steered off axis away from several hot spots to improve electron beam uniformity for the emittance measurements reported below.

Significantly less variation was observed on the Cu cathode. The rms QE variation for the Cu cathode was only 11% of the average QE. The minimum and maximum were 76% and 125% respectively of the average QE.

Longitudinal Emittance

Emittance measurements were made downstream of a 3 m SLAC linac structure located approximately 90 cm downstream of the cathode. The longitudinal emittance was determined by measuring the energy spread

downstream of a spectrometer magnet as a function of linac phase [2]. The technique is analogous to a quad scan for the transverse emittance measurements. A relatively large energy spread exiting the gun was observed for both cathodes. As expected there is not a significant difference in the longitudinal phase space with the Cu and Mg cathodes.

Table 2 lists the electron beam longitudinal parameters. All parameters were determined from a standard linear least square error fitting routine. The emittance and uncorrelated energy spread listed in Table 2 are overestimated due to non-linear energy-time correlation terms. Better estimates of the uncorrelated energy spread can be determined using tomographic phase space reconstruction [9]. With the actual beam phase space distribution the true slice energy spread can be calculated as opposed to the beam envelope which includes non-linear correlated terms.

Table 2: Longitudinal Beam Parameters at Linac Entrance.

Parameter	**Cu**	**Mg**	**Units**
Emittance	2.5	2.8	keVps
Normalized Emittance	1.5	1.7	μm
Bunch Length	0.44	0.41	ps
Energy Spread	36	48	keV
Uncorrelated Energy Spread	5.7	6.9	keV
Linear Correlation	-81	-120	keV/ps

Slice Emittance

The transverse slice emittance is measured using a quadrupole scan technique on the identical screen used in the longitudinal emittance measurements. Since the screen is in a dispersive section, the linac phase can be varied until the beam is sufficiently chirped at the screen that the beam can be temporally sliced into 10 beamlets. The energy-time calibration can be calculated since the longitudinal beam parameters are known at the linac entrance. The known beam matrix is propagated through the linac with the amplitude and phase settings used in the transverse emittance measurement and the resulting linear energy-time correlation is the calibration used to determine the time axis for the slice emittance measurements shown later.

For the transverse measurements a total of five beam parameters are fit in a least square fitting routine. In addition to the three Twiss parameters, the phase space offset with respect to the projection in both position and angle are also included. Thus a total of five parameters for each slice are measured which determine both the position and ellipse orientation in phase space. Previously we reported the slice emittance for the Cu cathode [10] and it is repeated here after correcting the beam propagation through the spectrometer. Also included are the slice emittance results from a Mg cathode for comparison. The phase space for all ten slices and the total projected emittance is shown in figure 2 for both cathodes.

The projected emittance is larger than the slice emittance largely due to the phase space offsets in both angle and position. The offsets are measured with respect to the projected centroid and thus are not due to steering errors but rather time dependent kicks. The kicks appear independent of charge so they are not due to wakefields. This suggests they originate at the gun or linac rf couplers [11]. The reversal of the head and tail with respect to the x axis between the two cathodes may be due to the different gradients used on the cathode, the different linac phase (Mg +19° and Cu +29°) or the fact that the beam was steered slightly off center for the Mg case due to the non-uniform electron emission. This will be investigated in more detail in later experiments.

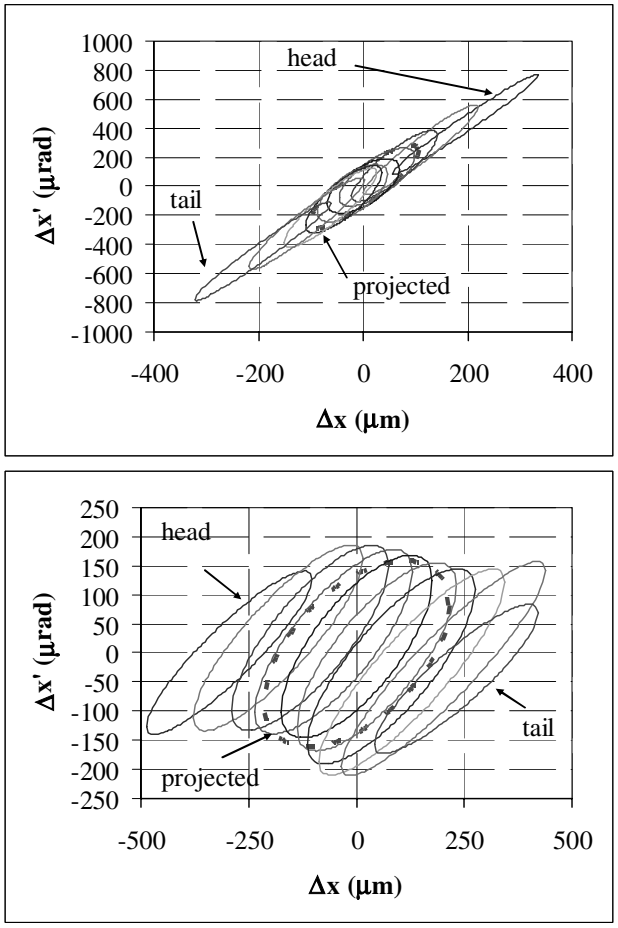

Figure 2: The upper plot shows the transverse phase space for the Cu cathode and the lower plot for the Mg cathode. The projected emittance is plotted as a red dashed line.

The minimum obtainable slice emittance is shown in figure 3 for both cathodes. The minimum emittance was obtained by measuring the emittance as a function of the emittance compensating solenoid field. It was determined empirically that the minimum emittance occurs when the solenoid focal length is adjusted to produce a waist near the linac exit.

The minimum slice emittance for the Cu cathode is approximately 0.6 μm while the Mg cathode is higher with 1.1 μm. The Cu results are in agreement with two other Cu cathode measurements at different laboratories using different techniques [12-13]. The measured values represent an upper limit for the thermal emittance from each cathode. The Mg cathode produces a higher emittance than the Cu cathode as expected although both values are approximately a factor of 2.5 times higher than the theoretical values listed in Table 1.

The emittance with the Mg cathode using a 0.5 mm radius cathode was also measured with approximately 20 pC charge and 11 A of peak current. The minimum emittance in this case was approximately 0.6 μm which is nearly half the value when the 1 mm radius laser was used. While this is consistent with the expected behavior due to thermal emittance (see equation 2) it is not conclusive that the measured emittance is equal to the thermal emittance. Experiments are underway to measure the projected emittance directly exiting the gun to better characterize the thermal emittance.

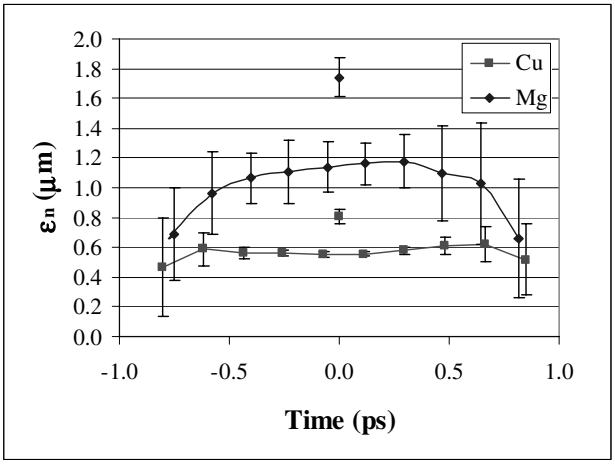

Figure 3: Emittance versus time for both the Cu and Mg cathodes. The projected emittance is plotted at t=0.

SUMMARY AND CONCLUSIONS

The transverse and longitudinal emittance in an S-band photocathode gun with a Cu and Mg cathode have been measured. No significant differences are observed in the longitudinal phase space. The minimum transverse emittance with a Cu cathode with 1 mm laser radius was 0.6 μm and 1.1 μm with the Mg cathode. The emittance from the Mg cathode decreased to 0.6 μm with a 0.5 mm radius laser spot size. These measured values set upper limits to the thermal emittance from Cu and Mg cathodes. The measurements are a factor 2.5 times larger than predicted by a theory that does not include temperature effects, surface roughness or electron-electron scattering. Only surface roughness can increase the theoretical emittance to the level of the measurements but it requires significantly roughened surfaces. It is more likely that a source of emittance growth in the gun or linac is contributing to the measured emittance. The time dependent position and angle offsets observed in the beam indicate the presence of a time dependent kick.

The QE was also measured from both cathodes. The Schottky effect is less pronounced with the Mg cathode due to the lower work function. The measured quantum efficiency with no laser cleaning is approximately $3\ 10^{-5}$ at 110 MV/m and 30° laser phase for the Cu cathode and $8\ 10^{-5}$ at 90 MV/m and 30° laser phase for the Mg cathode. No increase in QE for the Mg cathode was observed after scanning the cathode with an 800 μJ/mm^2 UV laser pulse.

ACKNOWLEDGEMENTS

The authors would like to acknowledge P. Pianetta for helpful discussions and the entire SSRL staff for helping to make this research possible. This work was supported by Department of Energy contract DE-AC02-76SF00515.

REFERENCES

[1] C. Limborg et al, NIM A528, (2004) 350-354.
[2] D. H. Dowell et al, NIM A507, (2003) 327-330.
[3] J.E. Clendenin et al, NIM A455, (2000) 198-201.
[4] R.C. Weast Editor, "CRC Handbook of Chemistry and Physics 1st Student Edition", (1988) E-78.
[5] S. Tanuma, C.J. Powell and D.R. Penn, Surface and Interface Analysis, Vol. 17, (1991) 911-926.
[6] M.J. Weber editor, "Handbook of Optical Materials", (2002) 317.
[7] E.D Palik editor, "Handbook of Optical Constants of Solids III", (1998) 239.
[8] D.R. Penn, Physical Review B, Vol. 35, No. 2, (1987) 482-486.
[9] H. Loos et al, NIM A528, (2004) 189-193.
[10] D.H. Dowell et al, Proceedings of the 2003 Particle Accelerator Conference, (2003) 2104-2106.
[11] D.H. Dowell et al, This conference, TUPOS56.
[12] W.S. Graves et al, Proceedings of the 2001 Particle Accelerator Conference, (2001) 2227-2229.
[13] J. Yang et al, Proceedings of the 2002 European Particle Accelerator Conference, (2002) 1828-1830.